Supplementary Information

Shared structural mechanisms of general anesthetics and benzodiazepines

Jeong Joo Kim[1], Anant Gharpure[1], Jinfeng Teng[1], Yuxuan Zhuang[2], Rebecca J. Howard[2], Shaotong Zhu[1], Colleen M. Noviello[1], Richard M. Walsh Jr.[3], Erik Lindahl[2,4] and Ryan E. Hibbs[1,*]

Affiliations:
[1]Department of Neuroscience, University of Texas Southwestern Medical Center, Dallas, TX 75390, USA
[2]Department of Biochemistry and Biophysics, Science for Life Laboratory, Stockholm University, Solna 17121, Sweden
[3]Department of Biological Chemistry and Molecular Pharmacology, Blavatnik Institute, Harvard Medical School, Boston, MA 02115
[4]Department of Applied Physics, Swedish e-Science Research Center, KTH Royal Institute of Technology, Solna 17121, Sweden
*Correspondence: ryan.hibbs@utsouthwestern.edu

Supporting Information Contents:

Supplementary video legends
Uncropped gel from Extended Data Fig. 1a
Expanded discussion of GABA alone, GABA plus flumazenil and GABA plus diazepam complexes
Expanded analysis and discussion of GABA plus picrotoxin and bicuculline complex structures

Supplementary video legends

Supplementary Video 1: Rocking movie to illustrate structural details of phenobarbital binding site at α-β interface.

Supplementary Video 2: Rocking movie to illustrate structural details of phenobarbital binding site at γ-β interface.

Supplementary Video 3: Rocking movie to illustrate structural details of etomidate binding site at one β-α interface.

Supplementary Video 4: Rocking movie to illustrate structural details of propofol binding site at one β-α interface.

Supplementary Video 5: Morphing movie between diazepam and flumazenil complex structures to illustrate conformational differences that give rise to the more expanded nature of the flumazenil complex.

Supplementary Video 6: Rocking movie of structural superposition of diazepam complex onto flumazenil complex, focusing on details of benzodiazepine site. Colored model is diazepam complex; flumazenil complex is in grey. Superposition was of principal (α) subunits at the α-γ interface.

Supplementary Video 7: Rocking movie to illustrate structural details of diazepam binding site at β-α interface.

Supplementary Video 8: Rocking movie to illustrate structural details of diazepam binding site at γ-β interface.

Supplementary Video 9: Cholesterol accumulation at protein-lipid interfaces. Representative converged snapshot of the GABA + phenobarbital model after 20 μs coarse-grained simulation in brain-lipid mixture, showing restrained protein subunits (α1, green; β2, blue; γ2, yellow) and proximal cholesterol molecules (cyan), viewed from the membrane plane. All other lipids are hidden for clarity.

Supplementary Video 10: Simulation and coloring as in Supplementary Video 5, showing proximal PIP_2 molecules (cyan).

Uncropped SDS-PAGE gel from Extended Data Fig. 1a:

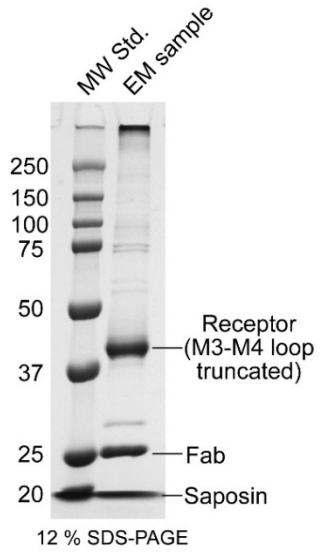

Expanded discussion of GABA alone, GABA plus flumazenil and GABA plus diazepam complexes

Here we expand on the brief description in the main text of three structures relating to diazepam potentiation and its inhibition by flumazenil. The reconstruction of the receptor in complex with GABA plus flumazenil in nanodiscs was initially resolved to 3.2 Å (Extended Data Figs. 2-4, 6, 7). Comparison of the ECD between this structure and the same complex in detergent[1] reveals near perfect agreement in protein structure and ligand positions (Extended Data Fig. 6f, g). As observed with the anesthetic complexes, but to an even larger degree, density for the γ-TMD was significantly weaker than for other subunits (Extended Data Fig. 2e). This observation was reminiscent of what had previously been seen in detergent[1], where the γ-TMD either collapsed into the pore or was structurally disordered (Extended Data Fig. 1). We performed focused 3D classification on the γ-TMD to improve local signal, which resulted in a 3.5 Å overall resolution map with strong signal in the γ-TMD, and an approximately symmetric membrane domain (Fig. 3a, Extended Data Figs. 2f, 3, 4). Closer investigation of the TMD revealed a prominent gap at the γ-β interface, with less surface area buried (635 $Å^2$) than the average of other interfaces (986 $Å^2$; Fig. 3d, Extended Data Fig. 6j). We were curious as to whether the presence of this gap was related to the presence of flumazenil, as it had not been observed in the anesthetic complexes, or in α1β3γ2 structures bound to classical benzodiazepines[2].

Initial processing of the GABA complex dataset revealed a disordered γ-TMD, similar to the flumazenil complex. Focused 3D classification yielded a 3.2 Å resolution map with strong signal for the γ-TMD (Fig. 3b, Extended Data Figs. 3-4 and Table 2). The ECD in the GABA alone complex overlays well with the GABA plus flumazenil complex, with nearly identical GABA binding sites (Extended Data Figs. 6h-i). The TMD is more compact (Fig. 3a, b), with the gap between γ and β subunits being smaller than in the flumazenil complex (919 $Å^2$ of buried surface area; Fig. 3d, e, Extended Data Fig. 6j). We next sought a point of comparison with a benzodiazepine with positive modulator activity. We selected diazepam due to its clinical prevalence, extensive functional characterization and the ability to compare our findings with recently published structures of the α1β3γ2 receptor type[2].

The γ-TMD of the diazepam complex was more clearly resolved than in both the GABA alone and the flumazenil-bound structures. The final reconstruction resulted from a 4-fold larger fraction of the particles than for the flumazenil complex and 2-fold larger than for GABA alone, revealing a correlation between presence of the positive modulator and conformational homogeneity (see Methods). This set of particles produced a 2.9 Å resolution reconstruction (Fig. 3c, Extended Data Figs. 3-4 and Table 2). The TMD of the diazepam complex is substantially more compact compared to the GABA alone and flumazenil-bound structures (Fig. 3a-f, Supplementary Video 5). The gap at the γ-β TMD interface observed in the flumazenil complex is closed, with surface area at the γ-β TMD interface, compared to the flumazenil complex, approximately doubled to 1103 $Å^2$ (Fig. 3d-f, Extended Data Fig. 6j). In addition to the expected density for diazepam at the classical benzodiazepine site in the ECD α-γ interface (Extended Data Fig. 7a, b), we observed three distinct densities for diazepam in the transmembrane domain, two at β-α interfaces observed previously[2] and a third at the γ-β interface that overlaps with one of the phenobarbital sites (Extended Data Fig. 7d-f, Supplementary Videos 7, 8). Binding of diazepam to this latter site may contribute to the overall stability of the TMD by closing the γ-β gap, similar to what was observed with the barbiturate, and may also play a role in benzodiazepine-induced potentiation through a mechanism similar to that of anesthetics[3,4].

We found that the γ-β site in the α1β3γ2 complex disfavors binding of diazepam because of the tighter packing of this interface (Extended Data Fig. 9k). While the TM helices of the two subunits overlap very well between the two structures, the π-helix on βM1 shows a substantial difference in its position. This essential component of the modulator site is shifted into the TMD cavity by approximately 1 Å compared to our model.

Consequently, the benzyl ring of diazepam as modeled in our complex would clash with γS280, γR284, βL223 and βQ224 (backbone carbonyl) in the α1β3γ2 complex. It is further possible that our incubation with diazepam during preparation of the membrane fraction and preparative gel filtration chromatography, rather than with the final material before making grids as for the α1β3γ2 structure, allowed for binding at the γ-β site.

Direct comparison between the flumazenil and diazepam complexes provides a structural context for understanding the two drugs' distinctive selectivities and functional properties. In the ECD α-γ interface, the benzodiazepine moiety of diazepam is flipped compared to flumazenil, with its pendant phenyl ring oriented away from the membrane and toward the principal subunit[2,5] (Extended Data Fig. 7b, c, Supplementary Video 6). Diazepam sits in the ECD pocket closer to the membrane than flumazenil, which results in unique contacts between the two ligands. Specifically, only diazepam contacts N60 on the complementary face, and only flumazenil interacts with T142 on the complementary (γ) face and T207 on loop C of the principal (α) face (Extended Data Fig. 7b, Supplementary Video 6). While flumazenil can bind to α-γ interfaces in a non-selective manner[6], diazepam does not modulate receptors via α4-γ or α6-γ interfaces, wherein the critical αH102, which may form a hydrogen bond with the chlorine of diazepam, is replaced with an arginine[7]. Notably, while flumazenil is an antagonist at the α1-γ2 site, its activity varies from strong potentiator at α4 and α6-containing receptors to a negative modulator at α5-containing receptors[8,9], and some substitutions at the α1 histidine position (e.g. to F, K and E) convert flumazenil into a partial agonist[10]. The delicate dependence of flumazenil activity on the chemistry at the α-γ interface is consistent with its effects at the α1β2γ2 receptor being more complex than simply acting as an inert benzodiazepine-site competitor. These effects include global destabilization of the receptor, particularly in the γ2-TMD, as observed in the structure.

$GABA_A$ receptors harbor diverse modulatory sites in their TMD subunit interfaces, as identified by affinity labeling[11], mutagenesis[12,13], functional experiments[14] and recently structural biology[2,15-17]. In the presence of low concentrations of GABA, diazepam produces biphasic potentiation of the α1β2γ2 receptor[3]. The high-affinity site is at the well-defined α-γ interface in the ECD. Affinity-labeling and mutagenesis studies suggested that low-affinity sites exist at subunit interfaces in the TMD, in positions that overlap at least in part with binding sites for IV and volatile anesthetics[3,4]. Recent structures of the α1β3γ2 receptor identified diazepam bound at β-α interfaces in the TMD[2]. Our study confirms the presence and location of these sites, with residues identified by mutagenesis[3] directly interacting with diazepam molecules (Extended Data Fig. 7d, e, Supplementary Video 7). We observe diazepam bound below the M2 15′ asparagine (N265) of the β subunit and I228 at the short π-helix within the M1 helix of the α subunit (Extended Data Fig. 7e). The benzyl ring of diazepam orients toward the β subunit and makes electrostatic contacts with N265, a key residue for *in vitro*[3,4] and *in vivo*[18-21] anesthetic effects, and forms stacking interactions with βF289. The phenyl ring of diazepam buries deep into the subunit interface and contacts residues on M2 helices of both β and α subunits (βT262 and αL269 as well as αP233 in the M1 helix). Surprisingly, we identified a new class of diazepam binding site at the γ-β TMD interface (Extended Data Fig. 7d, f, Supplementary Video 8), in which the diazepine ring pucker inverts, adopting an enantiomeric conformation (Extended Data Fig. 7g). In contrast to the β-α sites, the diazepam at the γ-β interface positions above γS280, homologous to βN265. In this pose, the pendant phenyl ring of diazepam points away from the channel axis and interacts with conserved phenylalanine (γF304) and proline (βP228) residues (Extended Data Fig. 7f). Consequently, the benzyl ring is located near the γM2 helix and the diazepine carbonyl oxygen forms a hydrogen bond with γT277. Investigation of the other intersubunit sites in the TMD revealed a weak tubular density at the α-γ interface, which likely corresponds to a lipid (Extended Data Fig. 5f, g). Lipids spontaneously and frequently occupy this position in MD simulations (Supplementary Videos 9-10), supporting the existence of an orphan site that does not respond to benzodiazepines or anesthetics[11]. The α-β TMD site shares sequence similarity with the γ-β site and has been

proposed to be an active binding site for benzodiazepines[3,4] and barbiturates[22]. However, instead of diazepam density, we observed extended tubular density consistent with occupancy by a lipid (Extended Data Fig. 5f, h).

Occupancy of four sites by diazepam results in global stabilization compared to the GABA alone complex, and especially compared to the flumazenil complex (Fig. 3a-f). Together, these three structures and the anesthetic-bound complexes display a correlation between receptor stability in the TMD and activity of the allosteric ligand. In contrast to the stabilization in the TMD observed with positive modulator complexes, flumazenil binding destabilizes the TMD and results in a slightly expanded ECD (Supplementary Video 5). In simulations of the flumazenil-bound and GABA-alone complexes, GABA frequently dissociated (Fig. 3g, Extended Data Fig. 7h). Conversely, GABA remained stably bound at both its binding sites in all simulations of the diazepam-bound complex, consistent with a positive allosteric effect of this modulator on GABA activation (Fig. 3g, Extended Data Fig. 7i). Diazepam stabilized the TMD, as monitored in rmsd of the pore-lining M2 helices relative to complexes with GABA alone and with flumazenil (Fig. 3h). We next performed simulations where we substituted flumazenil for diazepam at the ECD site, but preserved the TMD diazepams. Notably, we saw specific dissociation of diazepam from the γ-β site (Fig. 3i), which is consistent with our structure-based hypothesis that flumazenil binding in the ECD destabilizes this interface.

Taken together, structural and dynamic analyses reveal that both benzodiazepine and anesthetic positive modulators stabilize local and global organization of the receptor. Studies on localization show increased synaptic clustering in the presence of diazepam and increased receptor diffusion out of synapses in the presence of negative allosteric modulators[23]. Thus, modulator binding to receptors has consequences that extend beyond simply affecting stabilities of conformational states.

Expanded analysis and discussion of GABA plus picrotoxin and bicuculline complex structures

This expanded discussion is focused on two new α1β2γ2 structures that are similar to those published recently for the α1β3γ2 receptor[2]. This pair of competitive and non-competitive antagonist-bound α1β2γ2 structures, combined with the electrophysiological analysis of channel block, provides insight into interpretation of structural conformations and suggests delipidation during nanodisc assembly can constrain the receptor and obscure conformational transitions.

Brief analysis of bicuculline and GABA plus picrotoxin structures

We obtained 3.1 Å and 2.9 Å resolution maps of the α1β2γ2 receptor bound to bicuculline, and GABA plus picrotoxin, respectively (Extended Data Fig. 3, 4 and Tables 1, 2). In the bicuculline complex, we observed strong densities for the ligand in the orthosteric binding pockets at β-α interfaces (Extended Data Fig. 6d). As expected in the presence of an antagonist, relative to the GABA alone complex, loop C bends away from subunit the interface, and the whole β sandwich of each subunit's ECD tilts away from the central axis, with the most dramatic change occurring in the principal β subunits (Supplementary Fig. 1). These conformational changes result in a tilting of the Cys-loop and the β1-β2 loop, which directly interact with the M2-M3 loop in the TMD, to 'push' the ECD-ends of the M2 helices toward the central pore axis. Consequently, the M2 helices of this complex are straightened (more normal to the membrane) compared to the presumed desensitized-state structures in this study, with a hydrophobic gate at the 9' position (Extended Data Fig. 8g). This pore conformation typifies a resting or antagonist-bound state in the Cys-loop receptor family[24,25]. Indeed, principal component analysis (PCA) of the ECD of the bicuculline and various GABA-bound states mapped a dominant transition (80%) involving contraction of exterior loops around the orthosteric β-α binding site (Supplementary Fig. 2c); the dominant transition (72%) in the TMD involves contraction of the upper M2 helices, along with rotation with respect to the ECD (Supplementary Fig. 2b). Importantly, the pore profile aligns well with the α1β3γ2 structure with bicuculline (PDB code: 6HUK)[2], however the α1β2γ2 structure from the current study is wider at the top of the pore (Extended Data Fig. 8d-f). In comparison to other complexes in this study, we did not observe a gap in the TMD at the γ-β interface, and the buried surface area at this interface (1133 Å^2) was larger than in the GABA alone complex (919 Å^2). This observation suggests that the γ-β interface in the TMD is less compact in agonist-bound complexes.

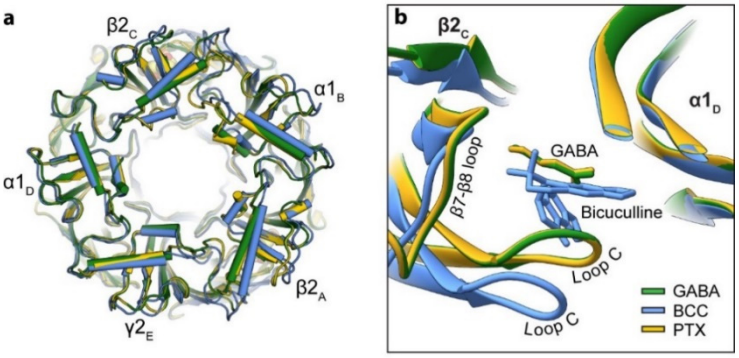

Supplementary Figure 1: Conformational difference between agonist and antagonist bound complexes. Panel **a** compares GABA, GABA plus picrotoxin, and bicuculline complexes in the extracellular domain. Panel **b** highlights the conformational difference at the orthosteric GABA binding site in three structures.

The GABA plus picrotoxin complex reveals an ECD conformation consistent with the GABA alone complex (an agonist-bound desensitized- or activated-state ECD), consistent with functional experiments showing no conformational changes in the ECD upon picrotoxin binding[26], and a distinct TMD conformation that appears intermediate between a desensitized state and resting state. Principal component analysis (PCA) finds that the TMD conformation of the picrotoxin complex lies at the midpoint of the path between resting and desensitized states (Supplementary Fig. 2b). In simulations of pore hydration, the upper half of the pore is hydrated in desensitized- and picrotoxin-bound states, but dehydrated in the resting, bicuculline-bound state (Supplementary Fig. 2a). Strong density for

picrotoxin was present between the 2′ and 6′ levels in the pore, with its hydrophobic isoprenyl tail oriented toward the cytosol (Extended Data Figs. 5e, 8d). This orientation, predicted from Monte Carlo simulations[27], results in favorable hydrophobic interactions at the 2′ position and electrostatic interactions at the 6′ position. The "tail-down" orientation is equivalent to that observed in the GluCl structure[28] (Extended Data Fig. 8e), but one α-helical turn up, consistent with cysteine labeling[29]. The orientation is flipped compared to the α1β3γ2 complex (PDB 6HUJ, Extended Data Fig. 8d)[2], which also sits slightly higher in the pore, perhaps due to the intracellular end of the pore being more tightly closed (Extended Data Fig. 9g-i).

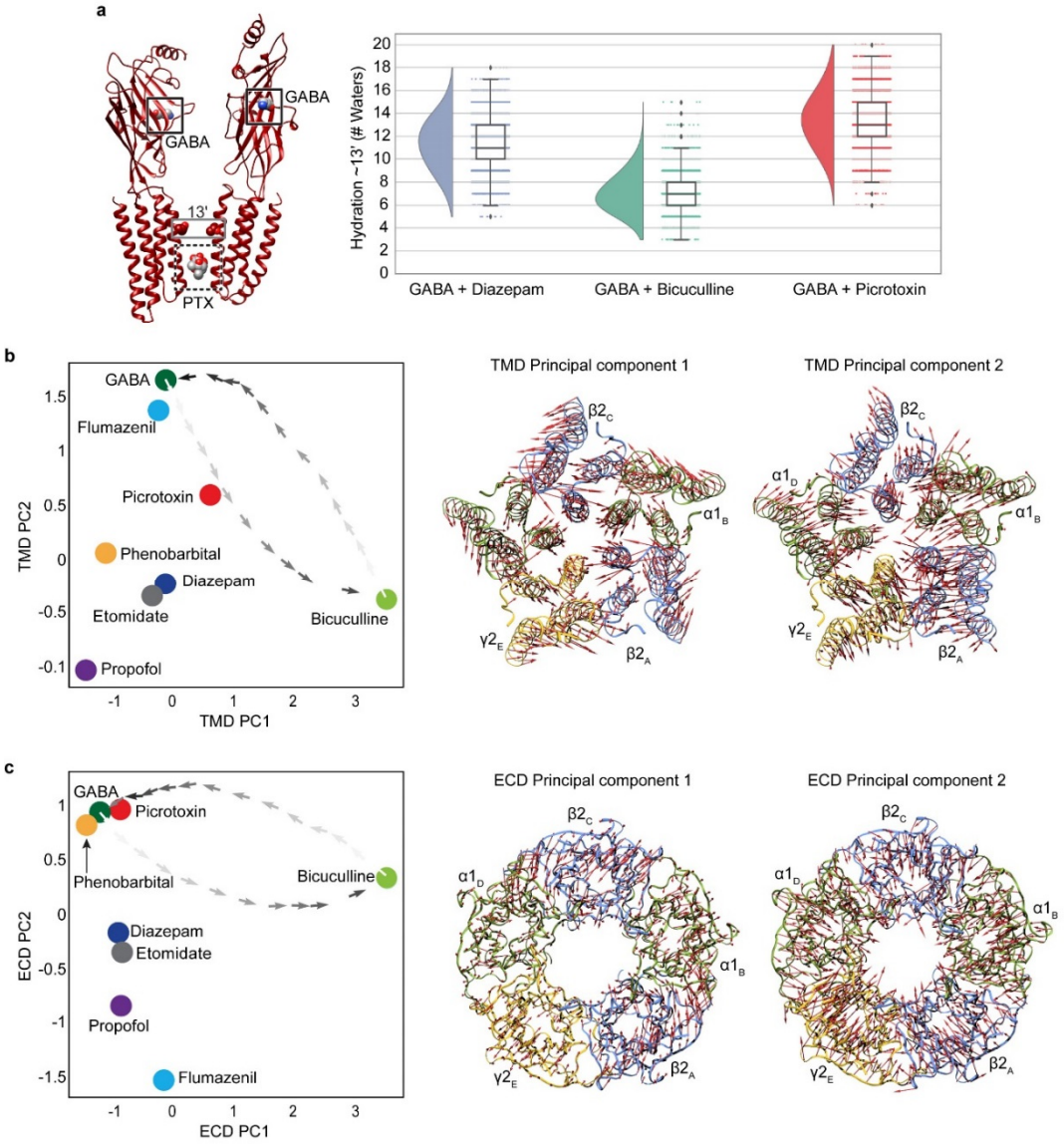

Supplementary Figure 2: Pore hydration and principal component analysis of α1β2γ2 $GABA_A$ receptor structures. Panel **a**, raincloud plots showing hydration above the hydrophobic gate (quantified by the number of water molecules associated with position 13′) in each frame of quadruplicate 500-ns simulations, with probability distributions at left, and raw data (n = 500 samples from 4 simulations, see Methods) plus boxplots indicating sample median, interquartile range (25th-75th percentiles), minimum–maximum range, and outliers at right. Simulations of the bicuculline complex (green) dehydrate relative to GABA + diazepam (blue) or picrotoxin complexes (red). A reference model shows initial states, including GABA (black boxes), picrotoxin (dashed box), and region of calculated hydration (13′). Panels **b-c** show principal component analysis of structures reported in this work (n = 8 independent structures), focusing on the TMD or ECD. Panel **b**, projections onto dominant principal components calculated for the TMD. Snapshots of elastic-network interpolations[30] between the GABA and bicuculline complexes (light-to-dark gray) show the GABA plus picrotoxin complex maps along this pathway. Models at right show the dominant principal component (72%) of the TMD ensemble

corresponds to symmetric motions associated with gating, including rotation of the TMD and inward translation of the upper M2–M3 region; the second component (15%) represents asymmetric expansion of the TMD, with opposing β and γ subunits moving apart as α subunits move toward one another. Panel **c**, projections as in **b** onto principal components calculated for the ECD. Models at right show the dominant principal component (80%) of the ECD ensemble corresponds to contraction of exterior loops around the orthosteric (β-α) binding site, while the second (16%) represents contraction of the ECD β-sandwiches.

Physiology and structural analysis to probe conformational states

Picrotoxin is a mixture of two compounds, picrotin and picrotoxinin. Picrotoxinin is the more active component and for simplicity we refer to it here as picrotoxin. This active component is what we built into the structural model. It is a natural product that has convulsant activity and plugs the channel of anionic Cys-loop receptor family members, the $GABA_A$ receptors and glycine receptors in humans. Myriad studies have been performed to characterize its mechanism of use-dependent channel block, and more specifically, the state(s) to which the toxin is thought to bind (resting, open, desensitized, an intermediate, or a combination)[13]. Picrotoxin is a rare example of a channel blocker whose binding is not voltage dependent[31], which makes it particularly useful in structural analysis, where there is no membrane potential to drive its binding. Recent electrophysiology combined with computational modeling[32] and an in-depth review on desensitization[25] present emerging consensus points about picrotoxin mechanism as it relates to receptor conformational selectivity. First, in order for picrotoxin to bind, the channel must open. In the sustained presence of GABA or glycine, picrotoxin will bind and physically occlude the ion pore. When it is bound, picrotoxin shifts the conformational equilibrium away from a desensitized state. After picrotoxin is bound, if the agonist is washed off, then picrotoxin can be trapped in the channel in a closed state. Assessing the conformational state of the receptor when picrotoxin is bound is challenging, as no current is present. However, voltage-clamp fluorometry experiments[33] show that in the presence of GABA, picrotoxin has little effect on the structure of the ECD, suggesting that while the conformation in the presence of GABA plus picrotoxin would not be desensitized, it would not be a simple resting state either.

We sought to place the structural conformation of the GABA plus picrotoxin-bound α1β2γ2 receptor in the context of functional experiments probing which conformational state(s) bind picrotoxin. For these experiments shown in Supplementary Fig. 3, we employed the same tri-cistronic expression plasmid used to produce protein for cryo-EM studies (see Methods), and whole-cell voltage clamp with transfected HEK cells. All recordings begin and end with application of a high concentration of GABA to illustrate absence of substantial rundown.

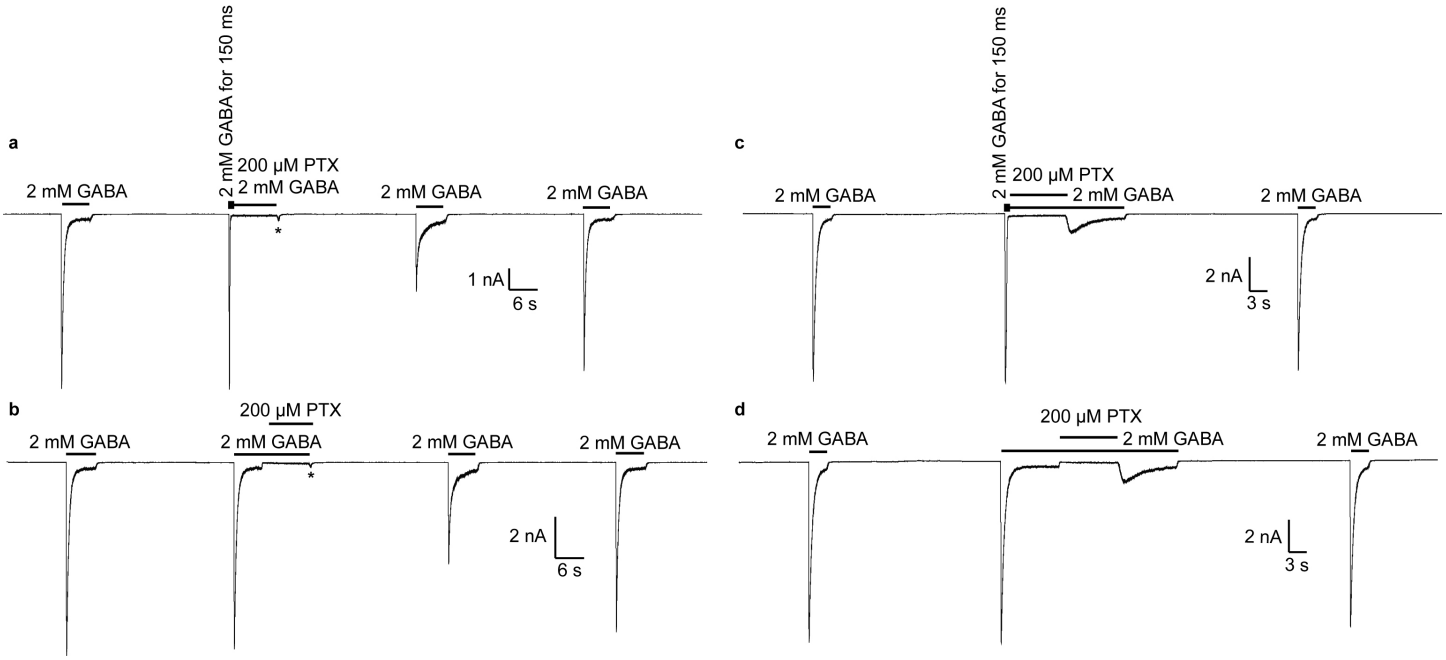

Supplementary Figure 3: Conformational dependence of pore block by picrotoxin

In **a**, 150 ms application of GABA opens the channel; this open channel is then rapidly blocked by picrotoxin in the sustained presence of GABA. Asterisk indicates small tail current, a hallmark of "foot in the door" blockers. Upon agonist washout, as they leave the pore, these blockers allow a small amount of residual current. The result is consistent with an open-channel block mechanism for picrotoxin, where when GABA is present, picrotoxin binds to and stabilizes the pore in an otherwise open, conducting conformation. Stabilizing an active conformation would be consistent with the well-documented loss in GABA affinity in the presence of picrotoxin[25], as GABA binds more tightly to a desensitized state than an open state. Subsequent application of GABA results in a partial response, which could be due to either a trapping block mechanism where picrotoxin was stuck in a closed pore, and required GABA application to allow it to exit the pore, or, alternatively, the receptor did not recover completely from desensitization. The final GABA application reveals a recovery of ~maximal current response, which suggests that desensitization was not the issue, but rather picrotoxin had been trapped in the pore and required opening for washout before a full response could be observed. That GABA is required to allow for blocker washout suggests that in the presence of GABA the pore conformation is more open than a simple resting state.

In **b**, GABA was applied for long enough to achieve steady-state current following desensitization of the majority of the channels before application of picrotoxin. The small tail current was again observed upon picrotoxin washout. Subsequent application of GABA resulted in a partial response, as in **a**, a result that suggests picrotoxin may bind to both open and desensitized channel states, in addition to being trapped in a closed state in the absence of GABA. We next sought to probe the preference of picrotoxin for open vs. desensitized pore conformations.

In **c**, after rapid open-pore block by picrotoxin as in **a**, picrotoxin is washed out during a sustained application of GABA. The relatively low peak amplitude upon washout of picrotoxin is consistent with picrotoxin binding to, at least in part, a desensitized pore conformation. Noteworthy is that the peak current upon picrotoxin washout is several fold greater than the steady state current with GABA alone, suggesting that picrotoxin shifts the equilibrium toward the open state, and away from the desensitized state.

In **d**, a long application of GABA is used to desensitize the population of receptors before picrotoxin is applied, and washout of picrotoxin occurs during continuous application of GABA. The result is similar to that from **c**, and supports our hypothesis that picrotoxin can bind to both open and desensitized channels; in the presence of GABA picrotoxin shifts the equilibrium away from desensitization toward an open or activatable channel, but only partially; and in the absence of GABA, picrotoxin can be trapped in the closed channel. The patch clamp experiments were repeated 3 times independently.

The pore conformation observed in the α1β2γ2 structure with GABA plus picrotoxin is distinct from the structure in the presence of the competitive antagonist bicuculline, where the resting state gate is fully closed. The α1β2γ2 structural results appear to be consistent with conclusions from the functional experiments: in the sustained presence of GABA, picrotoxin stabilizes a majority non-desensitized conformation, but one that picrotoxin is able to dissociate from much more readily than it could from a closed state, where dissociation occurs only very slowly if at all. Published findings are consistent with picrotoxin rapidly dissociating in the presence of GABA[32]. A comparison of the bicuculline vs. GABA plus picrotoxin structures from this study are shown, adjacent to comparison of analogous structural complexes of the α1β3γ2 receptor[2], in Supplementary Fig. 4. The overall conclusion from this comparison is that we see large conformational differences between the bicuculline (higher affinity, methylated form) complex and the GABA plus picrotoxin complex, while the recent study on α1β3γ2 found no conformational difference in the TMD or ECD/TMD junction between three structures: bicuculline, GABA plus picrotoxin, and picrotoxin alone. An absence of difference in receptor conformation is inconsistent with the physiological studies on the two classes of compounds.

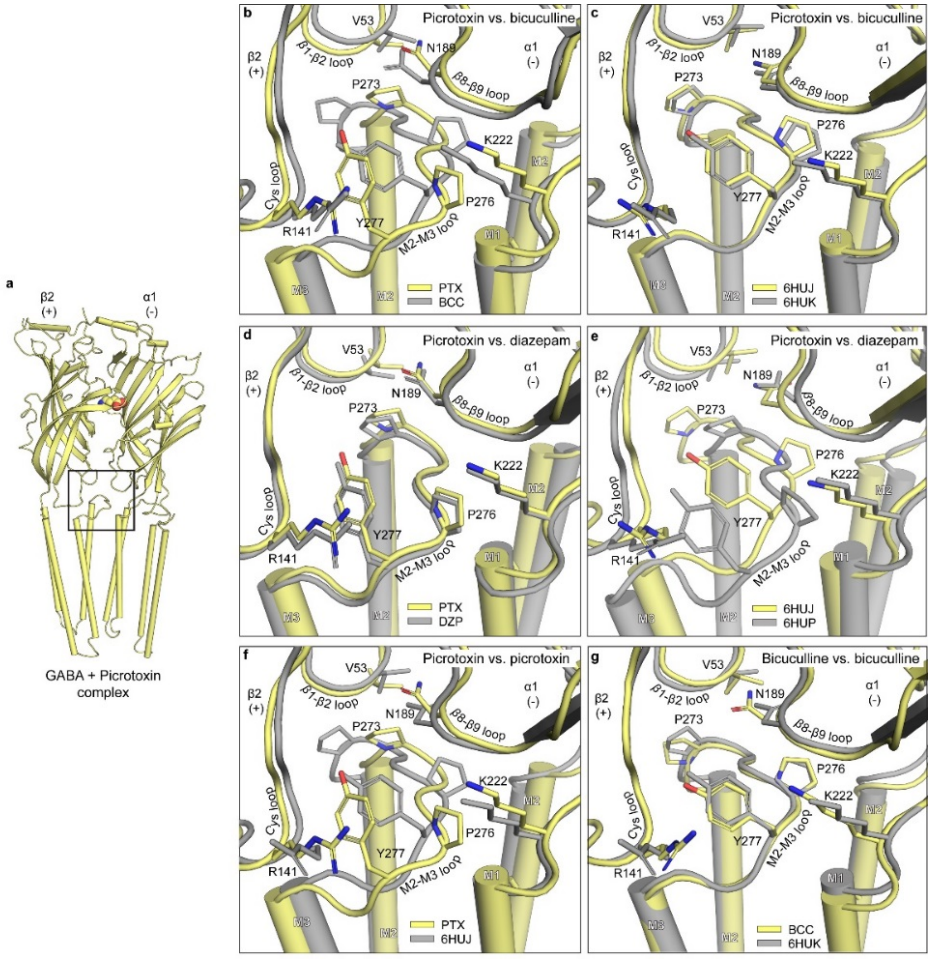

Supplementary Figure 4: Conformational differences among GABA plus picrotoxin, bicuculline, and GABA plus Diazepam complexes, at ECD-TMD junction, between α1β2γ2 and α1β3γ2 structures.
Panel **a** shows reference orientation of GABA plus picrotoxin complex. The ECD-TMD interface is indicated in a box. Panels **b** and **c** compare GABA plus picrotoxin complexes for the α1β2γ2 and α1β3γ2 structures, respectively. In α1β2γ2, the conformations are distinct: the ECD when GABA and picrotoxin are bound adopts a desensitized-like conformation, while the TMD adopts a conformation intermediate between a desensitized or open and a resting state conformation. In α1β3γ2, the conformations are ~equivalent for these two ligand complexes. In **d** and **e**, the same comparison is made but for GABA plus picrotoxin vs. GABA plus diazepam (desensitized). These two conformations are similar for α1β2γ2, and different for α1β3γ2. In **f** and **g**, each panel shows a comparison of the two receptors with the same ligand bound, illustrating that the two bicuculline complexes agree well, but the GABA plus picrotoxin complexes are strikingly different.

Caveats in the structural comparisons, and conclusions

As mentioned in the main text, there are important differences between the preparations for the structures we present in this study of the α1β2γ2 receptor, and those recently published of the α1β3γ2 receptor[2]. It is important to consider these differences when comparing structures. In addition to the reconstitution

approaches being fundamentally different, as described in the main text and Extended Data Fig. 10, the subunits and expression constructs are different. The sequence identity between full-length β2 and β3 is 82%. In the absence of the disordered (β3) or deleted (β2) ICD, the sequence identity is 92%. The pore-lining residues in the M2 helix are 100% identical. Only 6 residues are different within the TMD: one in M3 (M294 to L), 5 in M4 (all facing toward lipid, except F330 (to L: facing M3)). In the current study, the same intracellular loop truncation was used as in the first structural study on this receptor[1]. Removal of this intracellular loop dramatically boosts expression. This enhanced expression is essential to obtain the >5 mg/ml concentrations needed on the grid. Such a high concentration is needed because fluorinated detergent is added to the sample immediately before freezing EM grids to overcome a severe preferred orientation problem common among pentameric receptors that are not already in detergent. The presence of detergent results in most of the protein sticking to the carbon and avoiding the grid holes where images are collected; high protein concentrations allow for sufficiently high particle density in the grid holes.

The α1β3γ2 preparation utilized full-length subunit constructs; there, a nanobody was identified that allows for random receptor orientations on the grid without addition of detergent, a very useful tool. Absence of detergent allows for much lower protein concentrations to be added to the grid while still obtaining a high density of particles. Thus, the difference in construct could be responsible for differences in conformation, as could the different activities of the nanobody vs. the Fab fragment used in this study to facilitate particle alignment. It is beyond the scope of this study to formally rule out these possibilities. We think it unlikely, however, that the constructs and additives are the culprits.

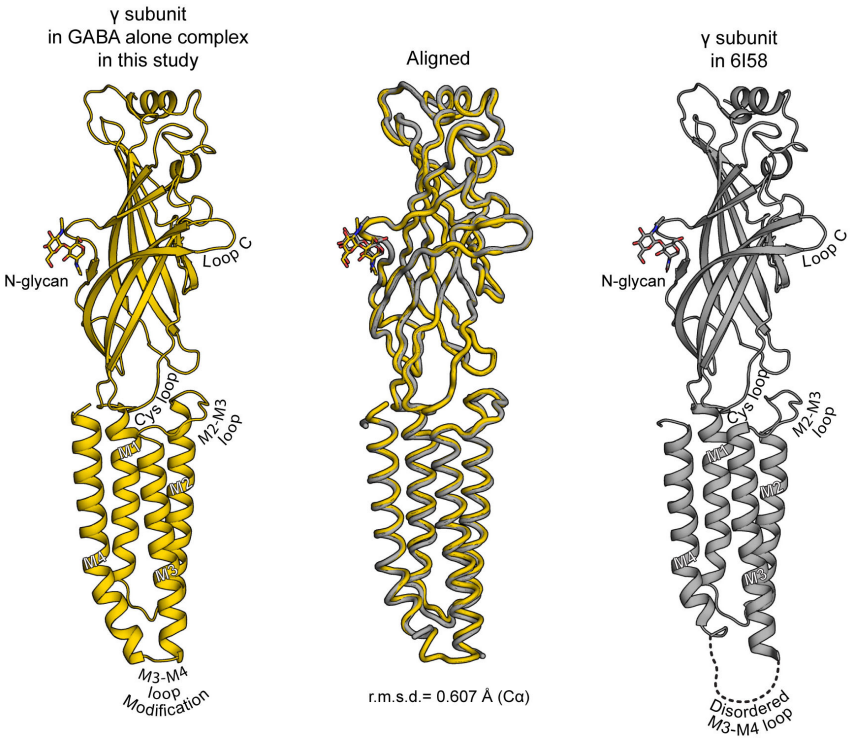

Supplementary Figure 5: **Superposition of γ2 subunits from the GABA complex in this study and from the 2019 α1β3γ2 receptor studies.** Left panel shows an atomic model of the γ2 subunit from the GABA alone complex in this study. The right-most panel shows the same subunit from the full-length α1β3γ2 receptor (PDB code: 6I58). The central panel shows a superposition of two γ2 subunits from two independent studies.

A recent study on the homologous glycine receptor found no conformational difference in the TMD when comparing structures of the full-length receptor to structures of the receptor with the M3M4 loop deleted[34]. Superpositions of the γ-TMD from this α1β2γ2 study with that from the α1β3γ2 structures reveal conservation in conformation of the helical bundle conformation (Supplementary Fig. 5). Functional comparisons between the truncated construct in this study and the WT construct revealed no differences (Extended Data Fig. 11 and reference[1]). The GABA + diazepam models from the two studies overlay very well in the extracellular domain, where the nanobody and Fabs bind. The transmembrane domains are also nearly identical (excepting the M3M4 loop); the systematic difference is that the pore is narrower at its extracellular end in α1β3γ2, far from the site of the M3M4 loop modification. If the M3M4 loop deletion had an effect on TMD conformation, that perturbation should instead be largest near the site of modification. A common feature among the structures is the relatively dynamic nature

of the γ2 subunit; it consistently has the highest relative atomic B factors among subunits, and in the α1β3γ2 structures, the least-resolved M3M4 loop residues.

This comparison provides confidence in both sets of structures. The consistent difference in the three structural points of comparison is in the tightness in the TMD packing and in the pore diameter; the α1β3γ2 receptor structures are all more tightly packed (Extended Data Fig. 9j). The difference in reconstitution approach, where the nanodisc belt tightens around the TMD upon removal of detergent, is a logical explanation for how this might occur (Extended Data Fig. 10). Considering, additionally, the asymmetric[1] and low local-resolution structures[35] in detergent, this trend suggests that the αβγ $GABA_A$ receptor is more sensitive to perturbations in its membrane environment than many other members of the Cys-loop receptor family. One reference example of another heteromeric pentameric channel whose structure has been characterized in both lipid and detergent is the α3β4 nicotinic acetylcholine receptor; in that case, the structures are equivalent[36].

Supplementary References

1 Zhu, S. *et al.* Structure of a human synaptic GABAA receptor. *Nature* **559**, 67-72, doi:10.1038/s41586-018-0255-3 (2018).

2 Masiulis, S. *et al.* GABAA receptor signalling mechanisms revealed by structural pharmacology. *Nature* **565**, 454-459, doi:10.1038/s41586-018-0832-5 (2019).

3 Walters, R. J., Hadley, S. H., Morris, K. D. & Amin, J. Benzodiazepines act on GABAA receptors via two distinct and separable mechanisms. *Nat Neurosci* **3**, 1274-1281, doi:10.1038/81800 (2000).

4 Middendorp, S. J., Maldifassi, M. C., Baur, R. & Sigel, E. Positive modulation of synaptic and extrasynaptic GABAA receptors by an antagonist of the high affinity benzodiazepine binding site. *Neuropharmacology* **95**, 459-467, doi:10.1016/j.neuropharm.2015.04.027 (2015).

5 Middendorp, S. J., Puthenkalam, R., Baur, R., Ernst, M. & Sigel, E. Accelerated discovery of novel benzodiazepine ligands by experiment-guided virtual screening. *ACS Chem Biol* **9**, 1854-1859, doi:10.1021/cb5001873 (2014).

6 Sieghart, W. & Savic, M. M. International Union of Basic and Clinical Pharmacology. CVI: GABAA Receptor Subtype- and Function-selective Ligands: Key Issues in Translation to Humans. *Pharmacol Rev* **70**, 836-878, doi:10.1124/pr.117.014449 (2018).

7 Wieland, H. A., Luddens, H. & Seeburg, P. H. A single histidine in GABAA receptors is essential for benzodiazepine agonist binding. *J Biol Chem* **267**, 1426-1429 (1992).

8 Yin, W. *et al.* Design, synthesis, and subtype selectivity of 3,6-disubstituted beta-carbolines at Bz/GABA(A)ergic receptors. SAR and studies directed toward agents for treatment of alcohol abuse. *Bioorg Med Chem* **18**, 7548-7564, doi:10.1016/j.bmc.2010.08.049 (2010).

9 Ramerstorfer, J., Furtmuller, R., Vogel, E., Huck, S. & Sieghart, W. The point mutation gamma 2F77I changes the potency and efficacy of benzodiazepine site ligands in different GABAA receptor subtypes. *Eur J Pharmacol* **636**, 18-27, doi:10.1016/j.ejphar.2010.03.015 (2010).

10 Dunn, S. M., Davies, M., Muntoni, A. L. & Lambert, J. J. Mutagenesis of the rat alpha1 subunit of the gamma-aminobutyric acid(A) receptor reveals the importance of residue 101 in determining the allosteric effects of benzodiazepine site ligands. *Mol Pharmacol* **56**, 768-774 (1999).

11 Forman, S. A. & Miller, K. W. Mapping General Anesthetic Sites in Heteromeric gamma-Aminobutyric Acid Type A Receptors Reveals a Potential For Targeting Receptor Subtypes. *Anesth Analg* **123**, 1263-1273, doi:10.1213/ANE.0000000000001368 (2016).

12 Mihic, S. J. *et al.* Sites of alcohol and volatile anaesthetic action on GABA(A) and glycine receptors. *Nature* **389**, 385-389, doi:10.1038/38738 (1997).

13 Olsen, R. W. GABAA receptor: Positive and negative allosteric modulators. *Neuropharmacology* **136**, 10-22, doi:10.1016/j.neuropharm.2018.01.036 (2018).

14 Krasowski, M. D. & Harrison, N. L. General anaesthetic actions on ligand-gated ion channels. *Cell Mol Life Sci* **55**, 1278-1303, doi:10.1007/s000180050371 (1999).

15 Laverty, D. *et al.* Crystal structures of a GABAA-receptor chimera reveal new endogenous neurosteroid-binding sites. *Nat Struct Mol Biol* **24**, 977-985, doi:10.1038/nsmb.3477 (2017).

16 Miller, P. S. *et al.* Structural basis for GABAA receptor potentiation by neurosteroids. *Nat Struct Mol Biol* **24**, 986-992, doi:10.1038/nsmb.3484 (2017).

17 Chen, Q. *et al.* Structural basis of neurosteroid anesthetic action on GABAA receptors. *Nat Commun* **9**, 3972, doi:10.1038/s41467-018-06361-4 (2018).

18 Jurd, R. *et al.* General anesthetic actions in vivo strongly attenuated by a point mutation in the GABA(A) receptor beta3 subunit. *FASEB J* **17**, 250-252, doi:10.1096/fj.02-0611fje (2003).

19 Reynolds, D. S. *et al.* Sedation and anesthesia mediated by distinct GABA(A) receptor isoforms. *J Neurosci* **23**, 8608-8617 (2003).

20 Zeller, A., Arras, M., Jurd, R. & Rudolph, U. Mapping the contribution of beta3-containing GABAA receptors to volatile and intravenous general anesthetic actions. *BMC Pharmacol* **7**, 2, doi:10.1186/1471-2210-7-2 (2007).

21 Zeller, A., Arras, M., Jurd, R. & Rudolph, U. Identification of a molecular target mediating the general anesthetic actions of pentobarbital. *Mol Pharmacol* **71**, 852-859, doi:10.1124/mol.106.030049 (2007).
22 Chiara, D. C. *et al.* Specificity of intersubunit general anesthetic-binding sites in the transmembrane domain of the human alpha1beta3gamma2 gamma-aminobutyric acid type A (GABAA) receptor. *J Biol Chem* **288**, 19343-19357, doi:10.1074/jbc.M113.479725 (2013).
23 Levi, S., Le Roux, N., Eugene, E. & Poncer, J. C. Benzodiazepine ligands rapidly influence GABAA receptor diffusion and clustering at hippocampal inhibitory synapses. *Neuropharmacology* **88**, 199-208, doi:10.1016/j.neuropharm.2014.06.002 (2015).
24 Nemecz, A., Prevost, M. S., Menny, A. & Corringer, P. J. Emerging Molecular Mechanisms of Signal Transduction in Pentameric Ligand-Gated Ion Channels. *Neuron* **90**, 452-470, doi:10.1016/j.neuron.2016.03.032 (2016).
25 Gielen, M. & Corringer, P. J. The dual-gate model for pentameric ligand-gated ion channels activation and desensitization. *J Physiol* **596**, 1873-1902, doi:10.1113/JP275100 (2018).
26 Muroi, Y., Theusch, C. M., Czajkowski, C. & Jackson, M. B. Distinct structural changes in the GABAA receptor elicited by pentobarbital and GABA. *Biophys J* **96**, 499-509, doi:10.1016/j.bpj.2008.09.037 (2009).
27 Zhorov, B. S. & Bregestovski, P. D. Chloride channels of glycine and GABA receptors with blockers: Monte Carlo minimization and structure-activity relationships. *Biophys J* **78**, 1786-1803, doi:10.1016/S0006-3495(00)76729-4 (2000).
28 Hibbs, R. E. & Gouaux, E. Principles of activation and permeation in an anion-selective Cys-loop receptor. *Nature* **474**, 54-60, doi:10.1038/nature10139 (2011).
29 Xu, M., Covey, D. F. & Akabas, M. H. Interaction of picrotoxin with GABAA receptor channel-lining residues probed in cysteine mutants. *Biophys J* **69**, 1858-1867, doi:10.1016/S0006-3495(95)80056-1 (1995).
30 Orellana, L. Large-Scale Conformational Changes and Protein Function: Breaking the in silico Barrier. *Front Mol Biosci* **6**, 117, doi:10.3389/fmolb.2019.00117 (2019).
31 Newland, C. F. & Cull-Candy, S. G. On the mechanism of action of picrotoxin on GABA receptor channels in dissociated sympathetic neurones of the rat. *J Physiol* **447**, 191-213, doi:10.1113/jphysiol.1992.sp018998 (1992).
32 Gielen, M., Thomas, P. & Smart, T. G. The desensitization gate of inhibitory Cys-loop receptors. *Nat Commun* **6**, 6829, doi:10.1038/ncomms7829 (2015).
33 Chang, Y. & Weiss, D. S. Site-specific fluorescence reveals distinct structural changes with GABA receptor activation and antagonism. *Nat Neurosci* **5**, 1163-1168, doi:10.1038/nn926 (2002).
34 Ivica, J. *et al.* The intracellular domain of homomeric glycine receptors modulates agonist efficacy. *J Biol Chem*, doi:10.1074/jbc.RA119.012358 (2020).
35 Phulera, S. *et al.* Cryo-EM structure of the benzodiazepine-sensitive alpha1beta1gamma2S tri-heteromeric GABAA receptor in complex with GABA. *Elife* **7**, doi:10.7554/eLife.39383 (2018).
36 Gharpure, A. *et al.* Agonist Selectivity and Ion Permeation in the alpha3beta4 Ganglionic Nicotinic Receptor. *Neuron* **104**, 501-511 e506, doi:10.1016/j.neuron.2019.07.030 (2019).